Field Precision LLC

Particle Trajectories in a Twisted Electrostatic Quadrupole Array

Field Precision LLC
E mail: techinfo@fieldp.com
Internet: https://www.fieldp.com

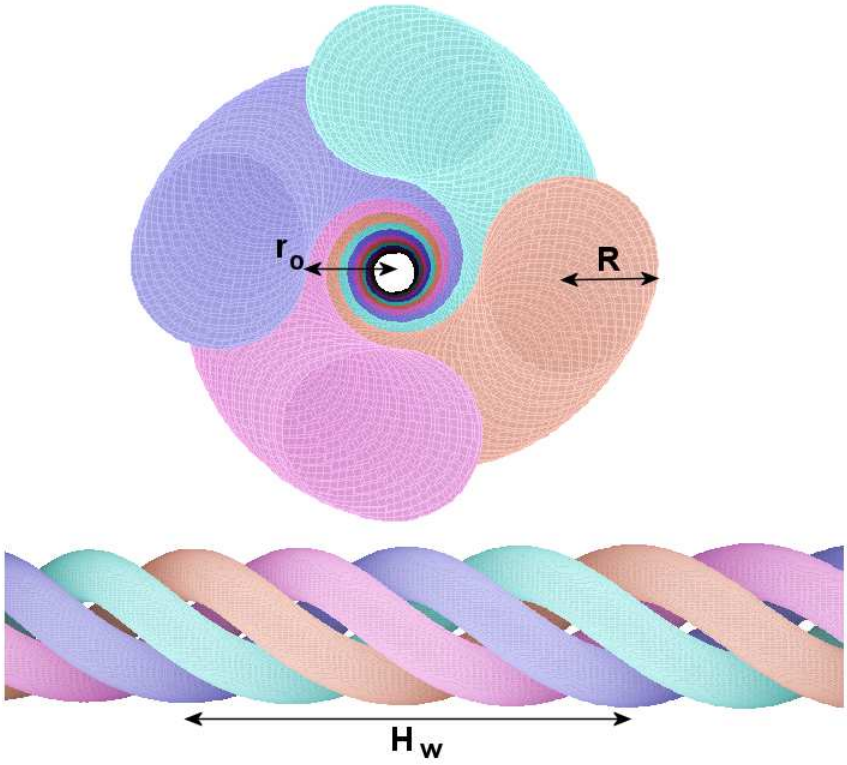

Figure 1: Geometry of a twisted electrostatic quadrupole focusing channel. Blue/Orange electrodes: $+V_o$, Red/Green electrodes: $-V_o$

This report introduces new features in the **OmniTrak** support utilities **Mapper** and **GenDist**. The capabilities will be illustrated with an example, a twisted electrostatic quadrupole channel for low-energy ion beam transport. The electrode geometry is shown in Fig. 1 shows the electrode geometry. A standard quadrupole array consists of individual lenses rotated by 90°. The difference is that the rotation in a twisted quadrupole occurs continuously. A potential application of the configuration is a differential pumping region between an ion source and an accelerator. Figure 1 defines geometric parameters. The bore radius (the minimum radial distance to an electrode) is r_o and the radius of a twisted rod is R. The period length, H_w, is equivalent to two FD focusing cells and contains the equivalent of four individual quadrupole lenses. The twisted quadrupole has some advantages over the discrete array:

- There are no gaps in the electric fields.
- Electrical and mechanical connections are required only at the ends.
- There is a small number of parts that can be largely self-supporting.
- The open structure is well suited to pumping.

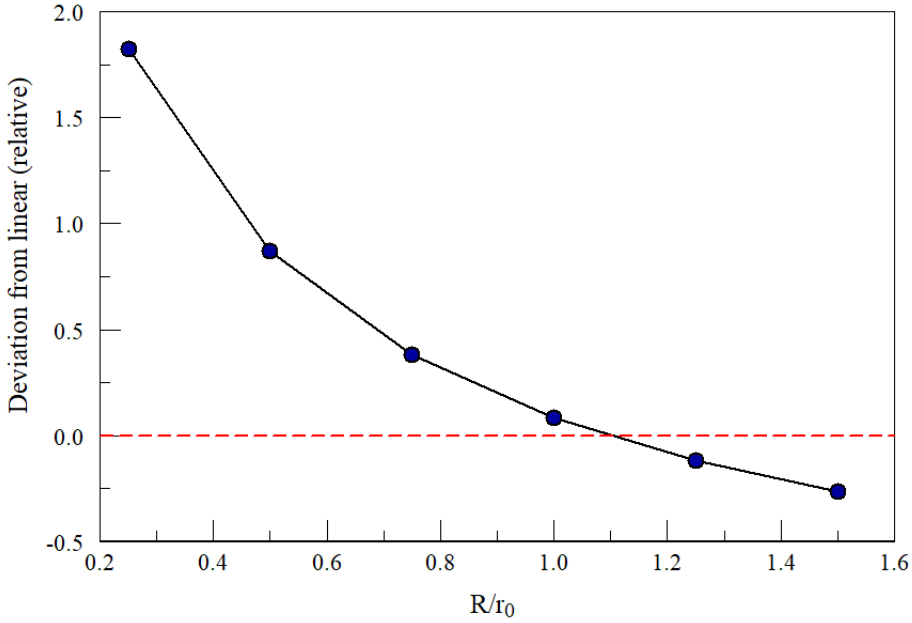

Figure 2: Quadrupole field formed by long circular rods of radius R a minimum distance r_o from the axis. Deviation from linearity over the bore as a function of R/r_o.

An initial issue is whether the rods shown in Fig. 1 give an accurate approximation to a quadrupole field. In theory, electrodes for an ideal field variation have hyperbolic cross sections. In this case, the electric field between the axis and electrode tip varies linearly. If the electrode mid-planes are aligned along the x and y axes, the field along the x-axis varies as:

$$E_x = \frac{2V_o x}{r_o^2}, \tag{1}$$

where the electrode voltages are $\pm V_o$. To check field variations with circular electrodes, calculations were performed with **EStat** for straight rods. The goal was to find the deviation from linearity as a function of the rod radius R for a given bore radius r_o. Figure 2 shows the results. The field was calculated at twenty points between the axis and pole tip and compared to the prediction of Eq. 1. The figure shows the radially-averaged fractional deviation. The choice $R = r_o$ was close to optimal and was used in the following calculations.

As a first step in an **OmniTrak** solution, a conformal mesh was created to represent a section of the transport system. The **MetaMesh** *HELIX* model is well suited to model the geometry. The example system had length 48.0 cm with $R = r_o = 1.0$ cm. In the **MetaMesh** script, this text represented a single electrode:

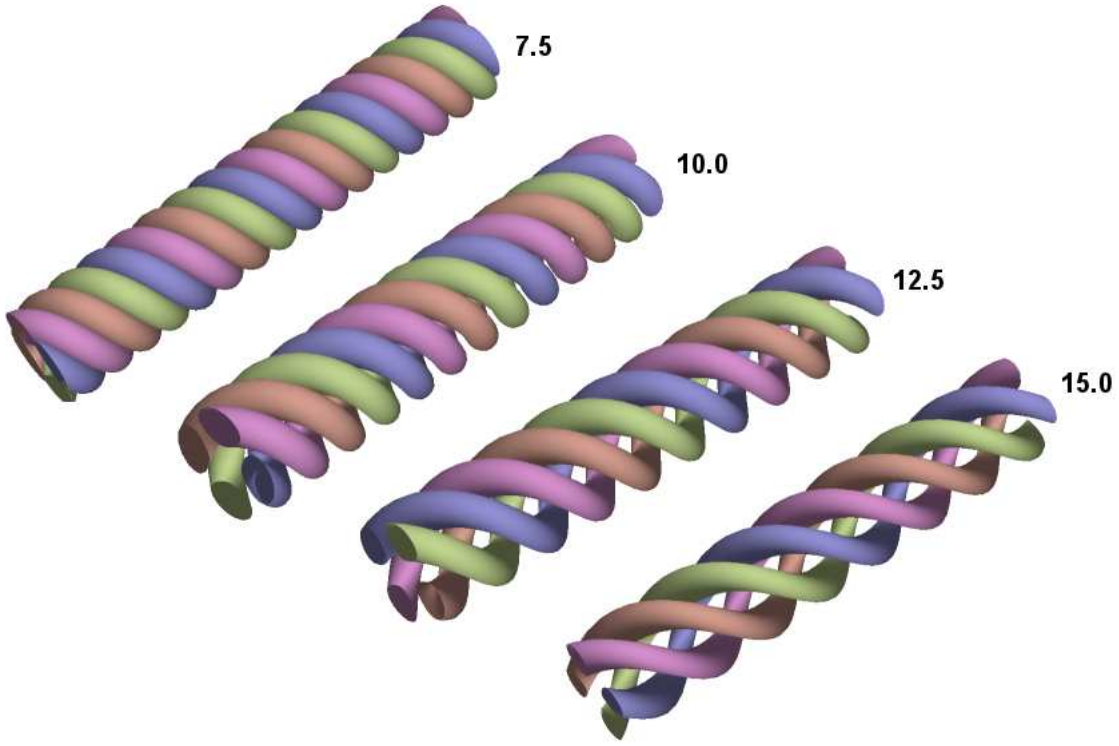

Figure 3: Twisted quadrupole configurations as a function of H_w/R for $R = r_o$.

```
PART
  Region: Q1
  Name: Q1
  Type: Helix
  Fab:   2.00000E+00  1.00000E+00  5.20000E+01  1.60000E+01
  Shift:   0.00000E+00  0.00000E+00 -4.00000E+00
  Rotate:     0.00    0.00    0.00  XYZ
  Surface Region Vacuum
END
```

The *FAB* command defines a helical rod of length 52.0 cm with radius $r_o = 1.0$ cm and axial period $H_w = 16.0$ cm. The rod center was at a distance $R + R_o = 2.0$ cm from the axis. The -4.0 cm displacement in the *SHIFT* command ensured that the electrodes were aligned with the x-y axes at $z = 0.0$ cm. In this case, the field variation would be directly comparable to that of Eq. 1. The other rods were assigned rotations about z of 90°, 180° and 270°.

A primary issue is a reasonable choice of the winding period H_w for a given rod radius R. Figure 3 shows a **Geometer** display of results for choices of Hw. Packing is too tight for $H_w \leq 10.0$. There would be significant axial field components with poor access for vacuum pumping. On the other hand, a large value would allow significant beam expansion in the defocusing direction with possible particle losses. The value $H_w = 16.0$ was used in following

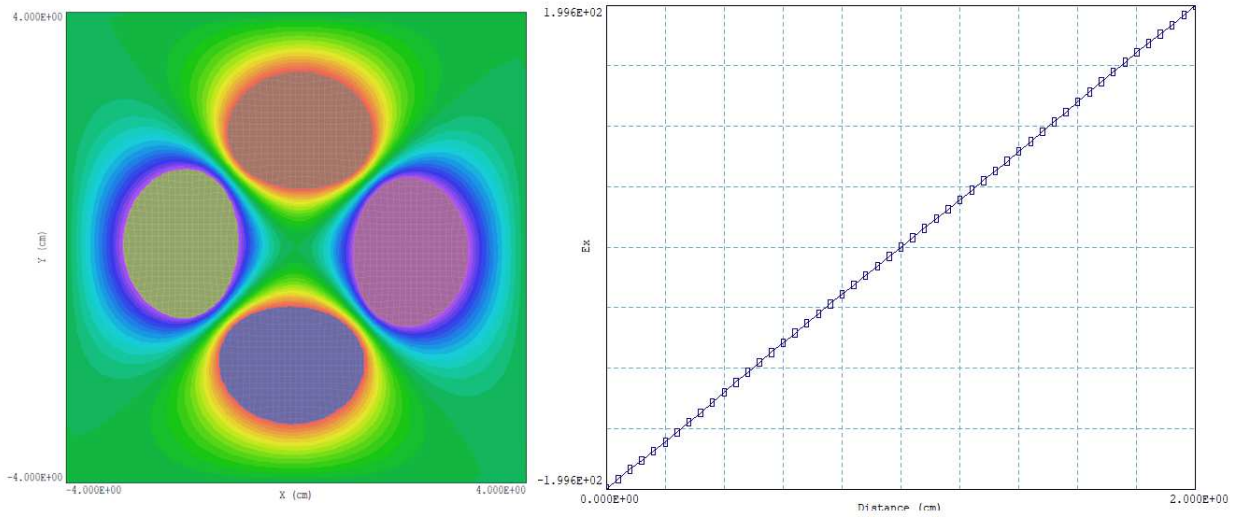

Figure 4: Electric fields of a twisted quadrupole with $R = 1.0$ cm, $r_o = 1.0$ cm and $H_w = 16.0$ cm in a grounded box with sides 8.0 cm. Applied voltages: ± 1.0 V. Left side: equipotential contours in the x-y plane. Right side: electric field scan along x at $y = 0.0$ cm.

calculations. In this case, an equivalent discrete lens array would have an FD cell length of 8.0 cm with an effective lens length of 4.0 cm (twice the bore radius).

The next step was the electric field calculation with **HiPhi**. The quadrupole array was enclosed in a grounded box of length 48.0 cm with widths 8.0 cm in x and y. The Neumann condition was applied at the entrance and exit boundaries ($z = 0.0$ and 48.0 cm) to approximate propagation in an infinite system. Voltages of ± 1.0 were applied to the rod pairs. In this case, Eq. 1 gives an electrode tip field of ± 200 V/m. The normalized solution was multiplied by a scale factor when loaded into **OmniTrak** to investigate voltage variations. Figure 4 shows results at $z = 24.0$ cm. The scan of E_x along the line $y = 0.0$ shows almost perfectly linearity with a tip field magnitude within 0.2% of the value for an ideal, non-rotating quadrupole.

The other input necessary for an **OmniTrak** simulation is a particle distribution. In response to the *PFILE* command, the program can load a set of particle parameters from a file. The file, with suffix *PRT*, contains one model particle per line. Each line specifies the particle mass, charge, kinetic energy, position and direction. The **GenDist** utility provides an efficient method to generate *PRT* files for large distributions. The program operates either interactively or under the control of a text script. There are several options for source shapes and angular distributions. We recently added the capability to create KV distributions[1] to model beams with emittance in order to make comparisons with standard transport calculations. The following **GenDist** script generates input for the present calculations.

[1]I.M. Kapchinskij and V.v. Vladimirskij, Proc. Intl. Conf. High Energy Accelerators, CERN, Geneva, 1959, p. 274.

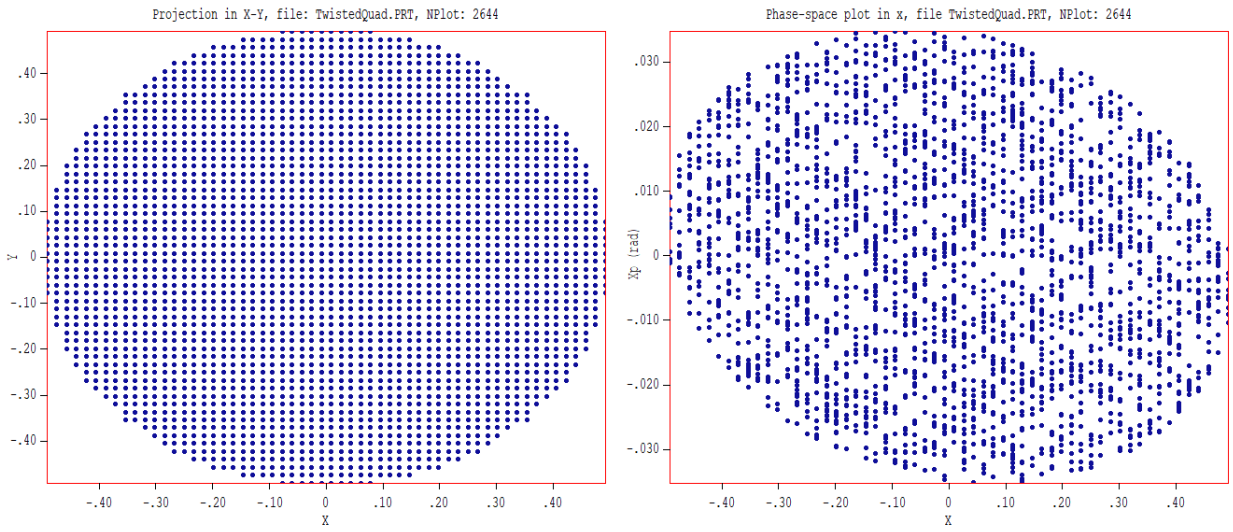

Figure 5: Input beam distribution. Left side: configuration space, distribution of model protons in x-y at $z = 0.0$ cm for a uniform flux. Right side: phase space distribution in x, converging beam with emittance.

```
FileType = PRT
RestMass =   1.0000E+00
Charge =   1.0000E+00
Energy =   5.0000E+04
Def(KV) = 0.5 0.5 2.0 2.0 2600
EnvAngle = -0.3 0.3
Distribution = Uniform
EndFile
```

The resulting beam consists of protons with kinetic energy 50.0 keV. The *DEF* command gives the source characteristics. The beam has an elliptical shape in the x-y plane with equal radii in x and y of 0.5 cm. The protons have a maximum angular divergence of $\pm 2.0^{\circ}$. The target number of model particles is 2600. The code algorithm seeks to fill the cross section with equally-spaced model particles, so the actual number is 2644. At the entrance point ($z = 0.0$), the quadrupole field is focusing in y and defocusing in x. As a starting point for a beam match, the beam is focused in x and defocused in y with respective envelope angles -0.3° and +0.3°.

Table 1 lists the script to control the **OmniTrak** run. The *EFIELD3D* command loads the normalized **HiPhi** solution and adjusts values by a multiplication factor. Several such lines are included and temporarily commented to carry out a scan of transport efficiency as a function of applied voltage. The *PFILE* command loads the particle input file created in **GenDist**. The *DUNIT* command signals that spatial quantities in `TwistedQuad.PRT` should be interpreted in centimeters. The file `TwistedQuadP.PRT` contains the parameters of particles that reach the exit or strike electrodes.

Table 1: Contents of file `TwistedQuad.OIN`.

```
FIELDS
*  EFIELD3D: TwistedQuad.HOU 0.0
*  EFIELD3D: TwistedQuad.HOU 500.0
*  EFIELD3D: TwistedQuad.HOU 1000.0
*  EFIELD3D: TwistedQuad.HOU 1500.0
*  EFIELD3D: TwistedQuad.HOU 2000.0
*  EFIELD3D: TwistedQuad.HOU 2500.0
*  EFIELD3D: TwistedQuad.HOU 3000.0
  EFIELD3D: TwistedQuad.HOU 3250.0
*  EFIELD3D: TwistedQuad.HOU 3500.0
*  EFIELD3D: TwistedQuad.HOU 4000.0
*  EFIELD3D: TwistedQuad.HOU 4500.0
*  EFIELD3D: TwistedQuad.HOU 5000.0
*  EFIELD3D: TwistedQuad.HOU 5500.0
*  EFIELD3D: TwistedQuad.HOU 6000.0
*  EFIELD3D: TwistedQuad.HOU 6500.0
*  EFIELD3D: TwistedQuad.HOU 7000.0
  DUNIT:   1.0000E+02
END
PARTICLES TRACK
  PFILE TwistedQuad
END
DIAGNOSTICS
  PARTFILE: TwistedQuadP
END
ENDFILE
```

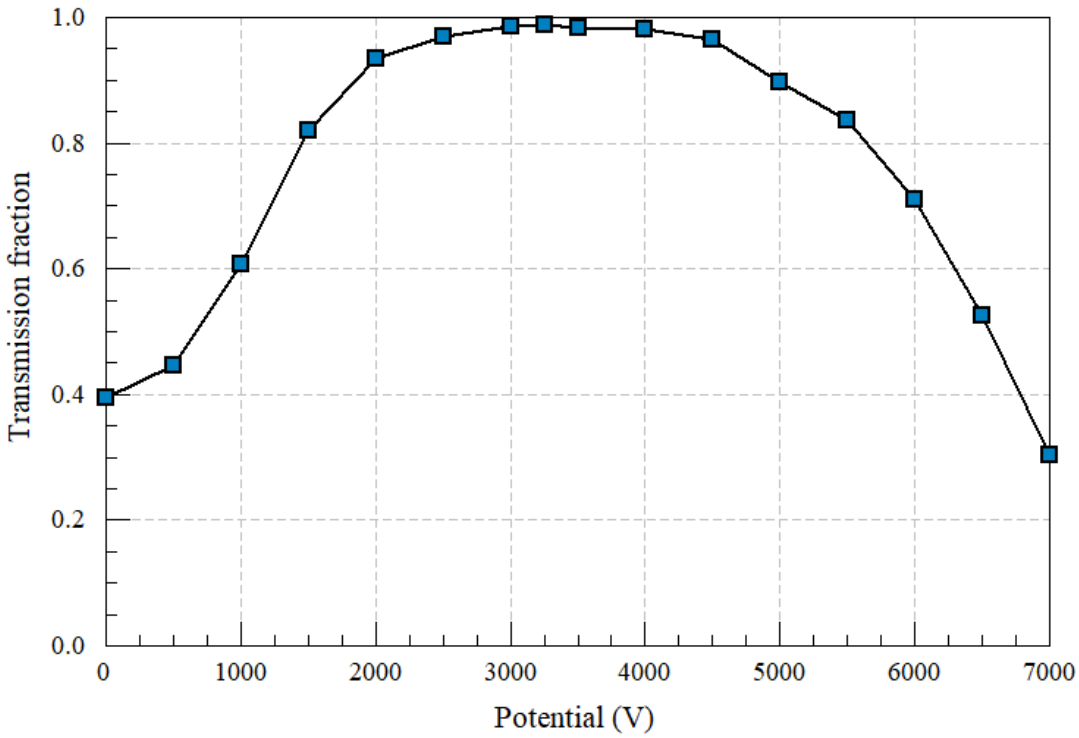

Figure 6: Transmitted fraction as a function of the electrode voltage.

Transport efficiency as a function of voltage was determined by making calculations with different field scaling factors. The transmission fraction for each run was determined by loading `TwistedQuadP.PRT` into **GenDist** and applying the filter $z \geq 47.9$ cm. Figure 6 shows the results. At low voltage the beam freely expands with particle losses on the electrodes. At high voltage the beam is over-focused with consequent losses. At 3250 V, the beam is approximately matched with 99% transmission. Figure 7 shows two views of the proton trajectories at this voltage.

The postprocessors **PhiView** and **MagView** can generate matrix files (maps) of three-dimensional field values from **HiPhi** and **Magnum** over portions of the solution volume. A matrix is a record of values of (E_x, E_y, E_z) or (B_x, B_y, B_z) projected on a simple regular mesh. The resulting text file is accessible to **OmniTrak** as well as outside software. Matrix files offer two advantages for particle tracking:

- Field interpolations are must faster on the regular mesh compared to the conformal meshes of **HiPhi** and **Magnum** solutions.

- Relevant portions of large-scale solutions can be extracted. For instance, an electron injector may be immersed in the field of a large magnet. A portion of the magnetic field can be represented efficiently over a detailed electric-field model space.

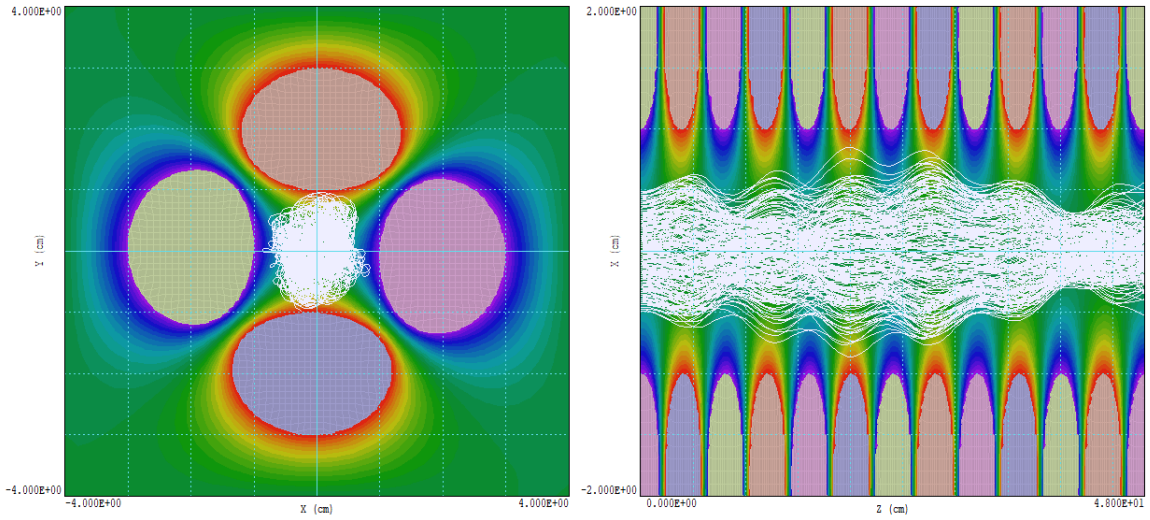

Figure 7: Proton trajectories with quadrupole electrode potentials ±3250 V. Left side. Projection in the x-y plane, true scale. Projection in the plane $y = 0.0$, expanded scale in x.

Mapper, a utility for analyzing and plotting matrix file data, is included in the **OmniTrak** suite. A new capability allows generation of matrix files from mathematical expressions. There are many possible applications that will be discussed in future reports. This report concentrates on representation of the twisted quadrupole configuration. Field values and proton trajectories are compared to the results of the finite-element solution. Figure 8 shows a coordinate system to derive expressions to approximate a twisted quadrupole field. The system x'-y' is rotated around z by an angle θ from the x-y axes. The transform is

$$x' = x\cos\theta + y\sin\theta, \tag{2}$$
$$y' = -x\sin\theta + y\cos\theta. \tag{3}$$

In the rotated frame, the quadrupole has the field components

$$E'_x = \frac{E_o x'}{r_o} = \frac{E_o}{r_o}(x\cos\theta + y\sin\theta), \tag{4}$$
$$E'_y = -\frac{E_o y'}{r_o} = \frac{E_o}{r_o}(-x\sin\theta + y\cos\theta). \tag{5}$$

where E_o is the electrode tip field magnitude. The transformation of the field components to the x-y frame is

$$E_x = E'_x\cos\theta - E'_y\sin\theta, \tag{6}$$
$$E_y y = E'_x\sin\theta + E'_y\cos\theta. \tag{7}$$

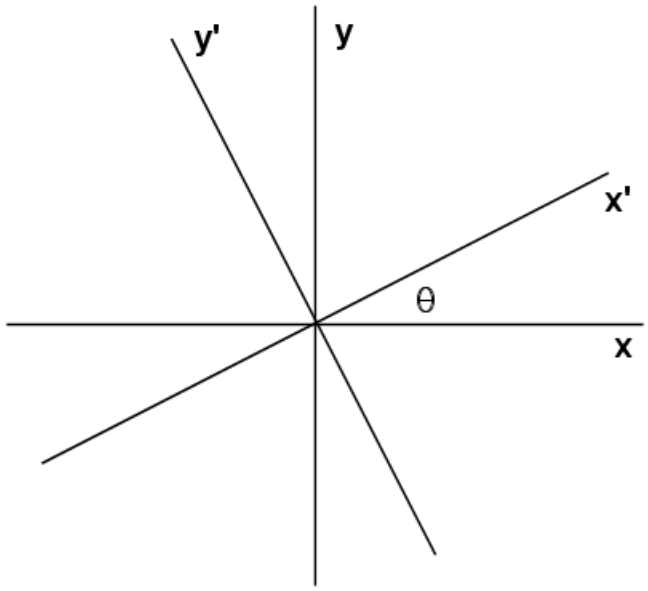

Figure 8: Coordinates for calculating the field components of a rotated quadrupole in planes normal to z.

Combining equations leads to the following expressions for the field components of a rotating quadrupole in the fixed frame:

$$E_x = \left(\frac{E_o}{r_o}\right) [\ x\ (\cos^2\theta - \sin^2\theta) + 2y\cos\theta\sin\theta\ ], \tag{8}$$

$$E_y = \left(\frac{E_o}{r_o}\right) [\ y\ (\sin^2\theta - \cos^2\theta) + 2x\cos\theta\sin\theta\ ]. \tag{9}$$

where $\theta = 2\pi z/H_w$.

Running **Mapper** and clicking the *Create table* tool opens the dialog of Fig. 9. The values shown apply to the current example. The solution box volume applies to the bore of the quadrupole array (-1.0 cm $\leq x, y \leq 1.0$ cm) and extends over the same length as the **HiPhi** calculation. The mathematical expressions for E_x and E_y correspond to Eqs. 8 and 9 in the **Mapper** syntax with an electrode tip field magnitude of $E_o = 200$ V/m. The **OmniTrak** input file has the content:

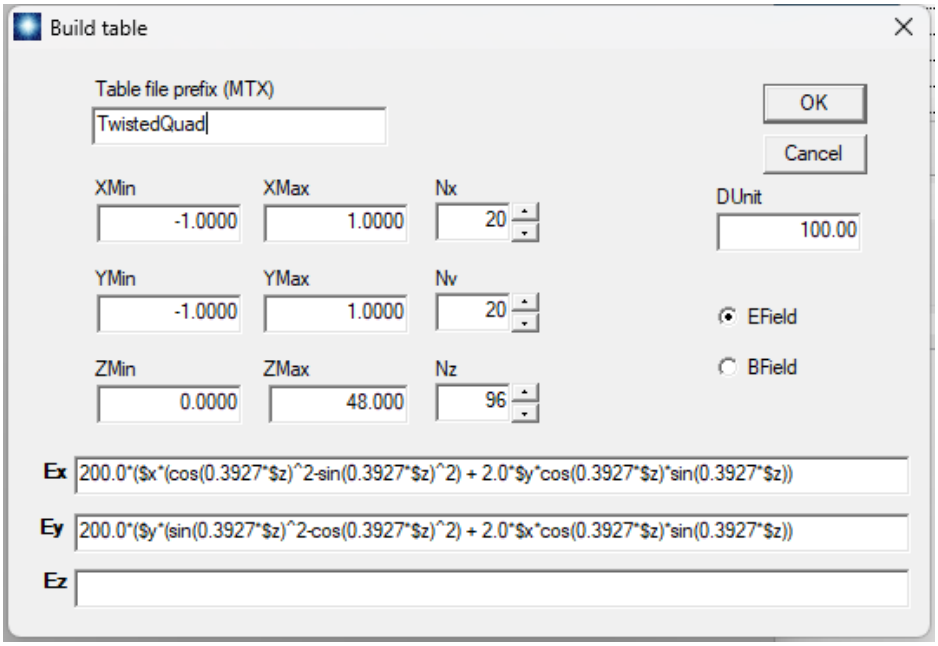

Figure 9: Mapper dialog for generating matrix files from mathematical expressions.

```
FIELDS
  ETABLE3D: TwistedQuad.MTX 3250.0
END
PARTICLES TRACK
  DUNIT:   1.0000E+02
  PFILE TwistedQuad
  DT:  0.50E-09
END
DIAGNOSTICS
  PARTFILE: TwistedQuadPFM
END
ENDFILE
```

The particle input file is the same as in the previous calculation. There are two differences: 1) loading and normalization of a field table rather than a finite-element solution and 2) explicit statement of the trajectory integration time step. Figure 10 shows trajectories projected to the plane y = 0.0 for an electrode voltage of 3250.0 V. The trajectories are almost identical to those of Fig. 7. Trajectories are terminated if they exit the volume of the field map. Although this condition differs from the exact representation of electrodes in the finite-element solution, the number of transmitted particles is close to that of the previous solution, 2603 compared to 2616. The plotting and analysis functions of **Mapper** can be used to confirm the validity of Eqs. 8 and 9. Figure 11 compares absolute values of E_x generated by **Mapper** to those calculated by **HiPhi**.

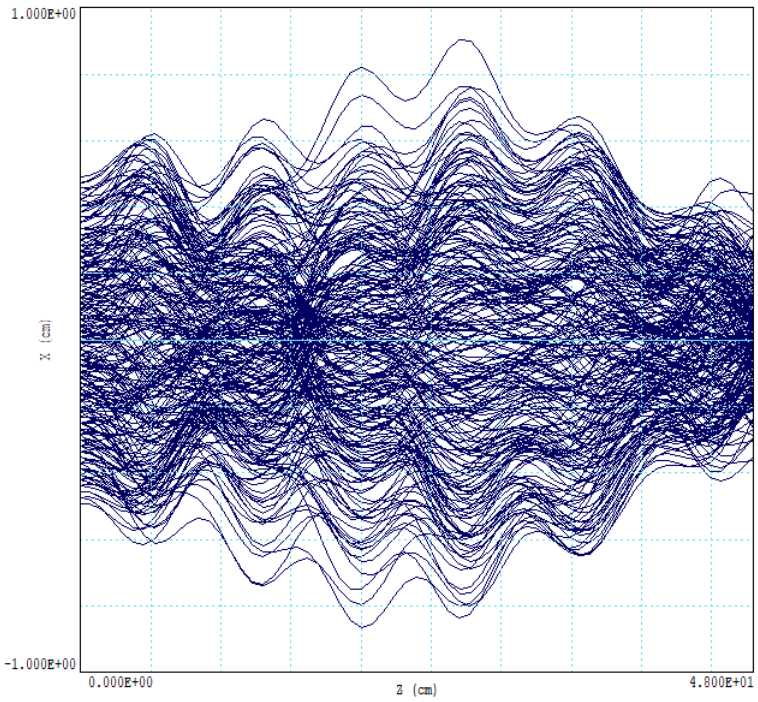

Figure 10: Field map calculation: proton trajectories projected to the plane $y = 0.0$ cm for an applied voltage 3250 V.

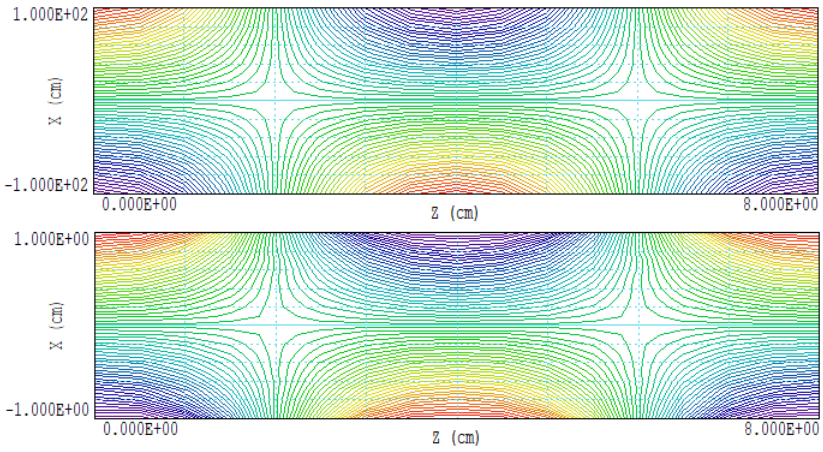

Figure 11: Comparison of field maps, plot of E_x in the plane $y = 0.0$ over the range $0.0 \leq z \leq 8.0$ cm with contours in the range -200.0 V/m $\leq E_x \leq +200$ V/m. Top: Generation by **Mapper** using the parameters show in Fig. 9. Bottom: Generation by **OmniView** from the full numerical solution with the same resolution and over the same region as the **Mapper** calculation.

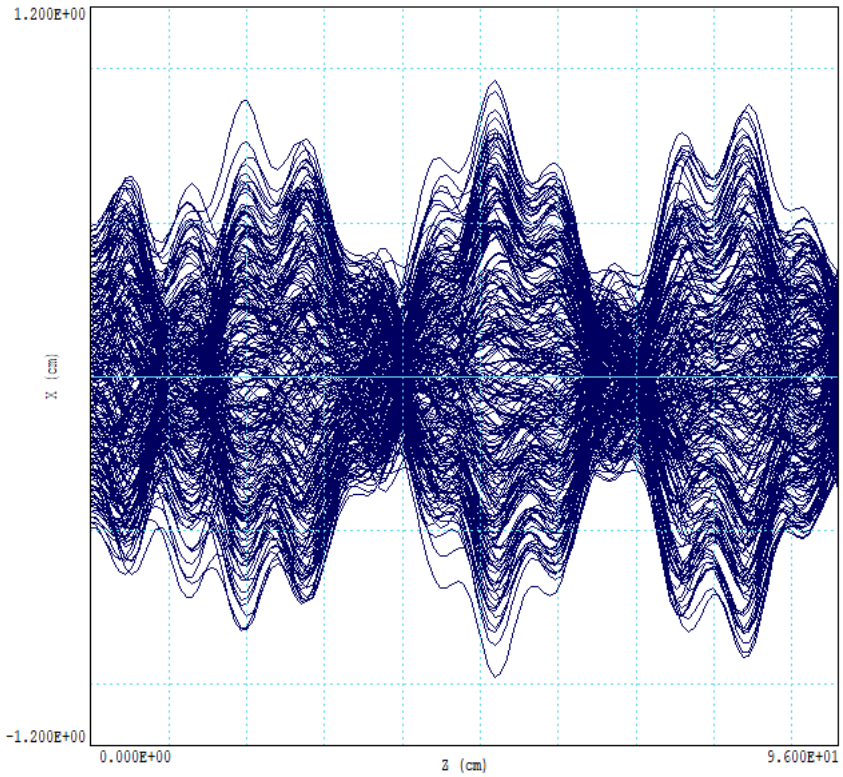

Figure 12: Electron trajectories projected to the plane $y = 0.0$ cm with a modified field map preserving the electric field magnitude. System length: 96.0 cm, twist period $H_w = 16.0$ cm, bore radius $r_o = 1.2$ cm, rod radius $R = 1.2$ cm, electrode voltage ± 3900 V.

When using field maps for trajectory calculations, it is relatively easy to investigate variations. For example, the length and bore of the twisted quadrupole can be adjusted by changing parameters in the dialog of Fig. 9. The system length is doubled by setting $Z_{max} = 96.0$ and $N_z = 192$. Consider increasing the bore width and rod radius to $r_o = R = 1.2$ cm while maintaining the same electric field amplitudes. The applied voltage should be increased from 3250 V to 3900.0 V. With the same period length $H_w = 16.0$ cm, the ratio H_w/R equals 13.3. Inspection of Fig. 3 indicates that the geometry is reasonable. With the changes, the **OmniTrak** calculation gives 100% transport efficiency over the full length. Figure 12 shows particle trajectories through the extended system.